

DOI: 10.1002/cmdc.201300343

# Discovery of MK-8742: An HCV NS5A Inhibitor with Broad Genotype Activity

Craig A. Coburn,<sup>\*[a]</sup> Peter T. Meinke,<sup>[a]</sup> Wei Chang,<sup>[e]</sup> Christine M. Fandozzi,<sup>[c]</sup> Donald J. Graham,<sup>[b]</sup> Bin Hu,<sup>[e]</sup> Qian Huang,<sup>[b]</sup> Stacia Kargman,<sup>[d]</sup> Joseph Kozlowski,<sup>[a]</sup> Rong Liu,<sup>[b]</sup> John A. McCauley,<sup>[a]</sup> Amin A. Nomeir,<sup>[c]</sup> Richard M. Soll,<sup>[e]</sup> Joseph P. Vacca,<sup>[a]</sup> Dahai Wang,<sup>[e]</sup> Hao Wu,<sup>[e]</sup> Bin Zhong,<sup>[e]</sup> David B. Olsen,<sup>[b]</sup> and Steven W. Ludmerer<sup>\*[b]</sup>

The NS5A protein plays a critical role in the replication of HCV and has been the focus of numerous research efforts over the past few years. NS5A inhibitors have shown impressive in vitro potency profiles in HCV replicon assays, making them attractive components for inclusion in all oral combination regimens. Early work in the NS5A arena led to the discovery of our first clinical candidate, MK-4882 [2-((S)-pyrrolidin-2-yl)-5-(2-(4-(5-((S)-pyrrolidin-2-yl)-1H-imidazol-2-yl)phenyl)benzofuran-5-yl)-1H-imidazole]. While preclinical proof-of-concept studies in HCV-infected chimpanzees harboring chronic genotype 1 infections resulted in significant decreases in viral load after both single-

and multiple-dose treatments, viral breakthrough proved to be a concern, thus necessitating the development of compounds with increased potency against a number of genotypes and NS5A resistance mutations. Modification of the MK-4882 core scaffold by introduction of a cyclic constraint afforded a series of tetracyclic inhibitors, which showed improved virologic profiles. Herein we describe the research efforts that led to the discovery of MK-8742, a tetracyclic indole-based NS5A inhibitor, which is currently in phase 2b clinical trials as part of an all-oral, interferon-free regimen for the treatment of HCV infection.

## Introduction

The World Health Organization (WHO) estimates that ~3% of the world's population are chronically infected with hepatitis C virus (HCV). Although HCV infection has both acute and chronic forms, most of the morbidity associated with infection is realized through the development of chronic liver disease in a subset of infected people years after initial acquisition of the infection.<sup>[1]</sup> HCV displays a high degree of genetic heterogeneity and can be classified into six major genotypes (GT1–6) and a series of subtypes (a,b,c,...), with genotypes 1a and 1b accounting for ~60% of all infections.

Current interferon-based therapy for chronic hepatitis C is limited by both efficacy and tolerability. Furthermore, the ability to achieve a sustained virologic response is largely dependent on the HCV genotype and duration of treatment. An im-

portant goal of future HCV therapy is to develop direct-acting antivirals in order to: 1) provide an all-oral interferon-free regimen, 2) decrease overall treatment durations, 3) provide broader coverage of HCV patient populations (e.g., GT2/GT3/GT4 infections, interferon-intolerant patients, and other difficult-to-treat populations), and 4) improve the overall safety and tolerability of HCV treatment regimens.<sup>[2]</sup> Given the propensity of HCV for generating genetic diversity, an interferon-free regimen will likely require two or more potent direct-acting compounds with non-overlapping resistance profiles in order to suppress the broadest-spectrum infections.

The HCV NS5A protein is a multifunctional RNA binding protein essential for viral replication. NS5A has no known enzymatic function, but has been shown to serve multiple functions at various stages of the life cycle, including viral replication and virion assembly.<sup>[3]</sup>

A landmark proof-of-concept study validated NS5A as a therapeutic target when it was demonstrated that a single dose of the NS5A inhibitor daclatasvir could effect a rapid virologic response in GT1-infected patients.<sup>[4]</sup> This result precipitated activity in the field and made NS5A a target for many research groups.<sup>[5]</sup>

Improvements in potency across a broad spectrum of HCV genotypes and mutants while maintaining favorable physical and pharmacokinetic parameters may lead to improved NS5A inhibitors with a higher barrier to resistance. Toward this end, a concerted research effort aimed at combining the structural components from both internal and literature compounds led to a series of potent NS5A inhibitors containing a central

[a] Dr. C. A. Coburn, Dr. P. T. Meinke, Dr. J. Kozlowski, Dr. J. A. McCauley, Dr. J. P. Vacca  
Department of Medicinal Chemistry, Merck and Company, Inc.  
West Point, PA 19486 (USA)  
E-mail: craig\_coburn@merck.com

[b] Dr. D. J. Graham, Q. Huang, Dr. R. Liu, Dr. D. B. Olsen, Dr. S. W. Ludmerer  
Department of Antiviral Research, Merck and Company, Inc.  
West Point, PA 19486 (USA)  
E-mail: steven\_ludmerer@merck.com

[c] Dr. C. M. Fandozzi, Dr. A. A. Nomeir  
Department of Preclinical Pharmacokinetics and Drug Metabolism (Merck)

[d] Dr. S. Kargman  
Department of In Vitro Pharmacology (Merck)

[e] W. Chang, Dr. B. Hu, Dr. R. M. Soll, Dr. D. Wang, Dr. H. Wu, Dr. B. Zhong  
Department of Medicinal Chemistry, WuXi AppTec  
Shanghai, 200131 China

indole or benzofuran scaffold from which advanced structures were derived. Herein we describe research efforts and highlight the preclinical properties of our first clinical NS5A inhibitor MK-4882, including efficacy studies in infected chimpanzees which ultimately led to the discovery of the current clinical compound MK-8742.

## Results and Discussion

Our initial efforts focused on the synthesis and SAR development of a series of *N*-arylpiperazines **1**.<sup>[6]</sup> The incorporation of a cyclic constraint within these structures afforded indole **2**, which showed similar potency in the replicon assay (GT1b EC<sub>50</sub> ~150 nM) and was an attractive entry toward modulating this target. Concurrent to these efforts, other NS5A inhibitors began to appear in the patent literature, but their SAR had not been fully delineated. Because of the structural similarity between compound **1** and the stilbene inhibitors **3**,<sup>[7]</sup> a lead-hopping effort was initiated with the goal of applying a similar cyclization strategy in order to explore the SAR of the pseudo-symmetric isosteres **4**. Subsequent reports revealed that compound **3** was also pivotal in the design of daclatasvir (Figure 1).<sup>[8]</sup>

Several heterocyclic scaffolds (**4a–4f**) were synthesized and incorporated into the final inhibitor structures. The cellular activity of each new compound was determined using the replicon-system-expressing genotypes 1b, 2a, and 1a. Initial results showed that benzimidazole **4a**, benzothiazole **4b**, and benzoxazole **4c** each had in vitro profiles worse than the parent stilbene inhibitor **3**, whereas benzofuran **4d** and indole **4e** had profiles similar to the reference compound. Alkylation of the

indole nitrogen atom resulted in a ~10-fold loss in replicon activities (**4f**), whereas the isomeric 2,6-disubstituted indole **4g** resulted in a substantial loss in potency relative to **4e**.

Within the context of the indole-based scaffold, replacement of the proline *N*-Cbz group by either the isosteric hydrocinnamate ligand (**5**) or an (*S*)-*N*-Boc-phenylalanine group (**6**) did not have a significant influence on potency. Synthesis and evaluation of the (*S*)-*N*-Boc-phenylglycine homologue **7** showed a 10-fold increase in genotype 1b and 2a potencies, while the epimeric (*R*)-*N*-Boc-Phg-containing diastereomer **8** afforded a 100–400-fold increase in GT1b and GT2a potencies and a 20-fold improvement in GT1a potency (Table 1).

Additional profiling of inhibitor **8** showed bioavailability to be low (<2%) in preclinical animals. The poor oral absorption of this compound was attributed to the high peptidic nature of the compound. To address this limitation, the C2'-phenyl amide bond was replaced by a variety of known amide isosteres (Table 2; X=oxazole, oxadiazole, pyrazole, thiazole). These modifications, however, resulted in compounds that displayed inferior replicon profiles relative to the parent amide **8**. Pyrazole analogue **11** appeared to have the best profile and it was speculated that the NH group was important for maintaining genotype 1a and 1b potencies. As such, imidazole **13** was synthesized, and whereas EC<sub>50</sub> values versus GT1b and 2a were similar to those of amide **8**, this modification resulted in a ~20-fold improvement in genotype 1a potency (EC<sub>50</sub>=3 nM).

Further exploration into the SAR of NH-containing heterocyclic amide isosteres resulted in the synthesis of the isomeric 2-propyl-5-phenylimidazole analogue **14**. This modification gave an additional ~20-fold increase in potency against GT1a while maintaining low-picomolar EC<sub>50</sub> values in the GT1b and GT2a

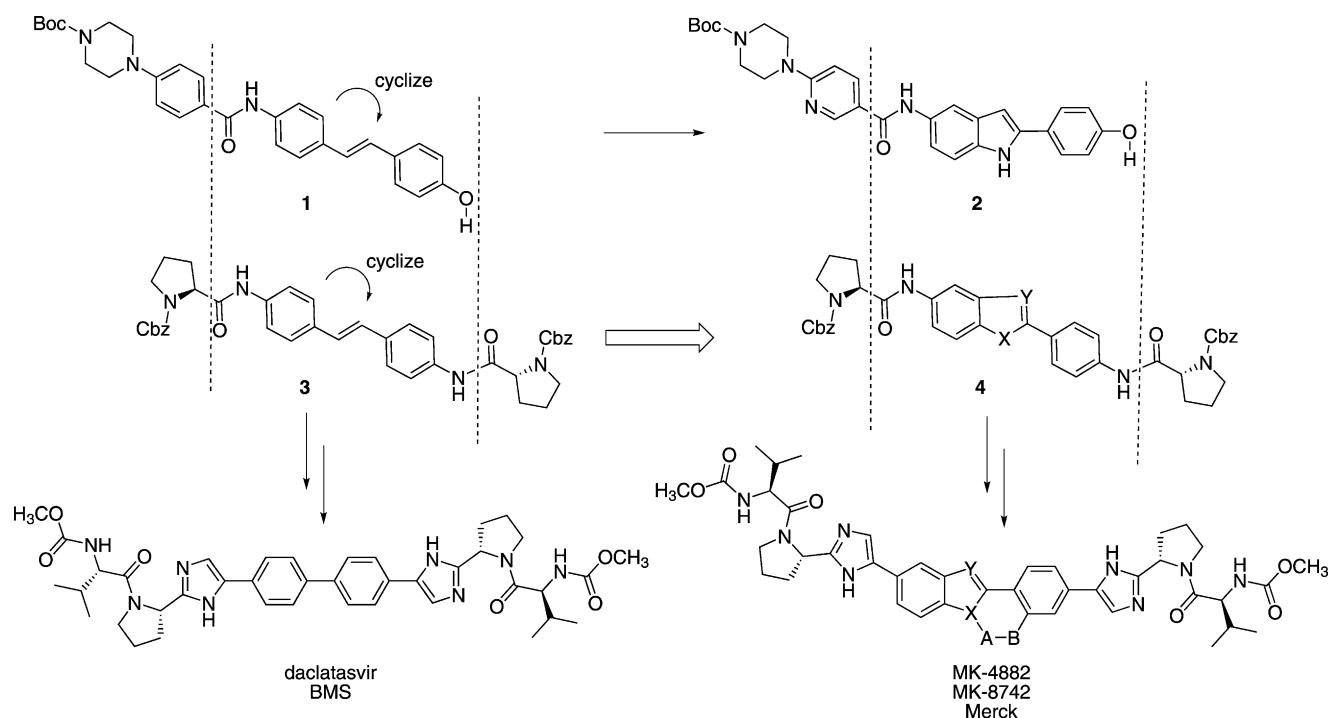
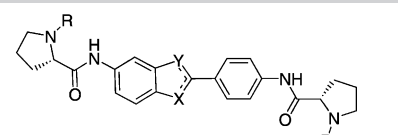


Figure 1. Strategy for the development of NS5A inhibitors.

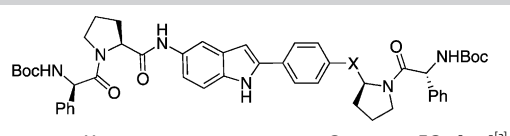
**Table 1.** Central scaffold SAR.



Compd	Substituent		Genotype, EC <sub>50</sub> [nM] <sup>[a]</sup>		
	R	X, Y	1b	2a	1a
<b>3</b>			5	60	> 20000
<b>4a</b>	Cbz	NH, N	> 20000	> 20000	> 20000
<b>4b</b>	Cbz	S, N	> 20000	> 20000	> 20000
<b>4c</b>	Cbz	O, N	160	1500	> 20000
<b>4d</b>	Cbz	O, CH	5	230	> 20000
<b>4e</b>	Cbz	NH, CH	16	290	1600
<b>4f</b>	Cbz	NCH <sub>3</sub> , CH	170	990	> 20000
<b>4g</b>	Cbz	CH, NH	> 20000	> 20000	> 20000
<b>5</b>	PhCH <sub>2</sub> CH <sub>2</sub>	NH, CH	4	290	2100
<b>6</b>	(S)-Boc-Phe	NH, CH	14	ND	ND
<b>7</b>	(S)-Boc-Phg	NH, CH	0.4	20	1500
<b>8</b>	(R)-Boc-Phg	NH, CH	0.004	0.05	70

[a] n ≥ 3; ND: not determined

**Table 2.** Amide isosteres.



Compd	X	Genotype, EC <sub>50</sub> [nM] <sup>[a]</sup>		
		1b	2a	1a
<b>8</b>	-NHC(O)-	0.004	0.05	70
<b>9</b>		0.44	500	> 266
<b>10</b>		0.09	86	> 266
<b>11</b>		0.016	1.3	47
<b>12</b>		0.2	26	> 266
<b>13</b>		0.01	0.07	3
<b>14</b>		0.01	0.015	0.17
<b>15</b>		0.06	> 266	150

[a] n = 3

replicon assays. The importance of the heterocyclic NH substituent was further proven by the loss in replicon potency of the N-methylated analogue **15**. Altogether, the incorporation of the imidazole amide isostere maintained both GT1b and 2a potency while improving GT1a potency by ~400-fold relative to the amide **8**.

Both single and double imidazole amide isosteres in the benzofuran series were prepared to further explore the effects

of the 2-prolyl-5-arylimidazole substitution on both potency and pharmacokinetics. Table 3 shows the results from imidazole incorporation first on the C5 benzofuran side (**17**; A=imidazole), then the C2' phenyl side (**18**; B=imidazole). In each case, genotype 1b and 2a potencies remained the same while genotype 1a potency improved by a factor of 10. Incorporation of both imidazole amide isosteres (**19**; A=B=imidazole) resulted in an additional 20-fold improvement in GT1a EC<sub>50</sub> values. On the basis of the low-picomolar EC<sub>50</sub> values in GT1a, 1b, and 2a replicon assays, compound **19** became an important lead. Subsequent research efforts focused on the SAR of the terminal amino acid groups in order to address the problematic oral absorption profile without perturbing the virologic profile.

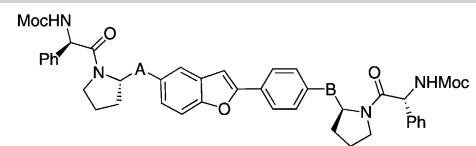
Table 4 shows the area under the curve (AUC) values after 10 mg kg<sup>-1</sup> oral dosing to fasted male Sprague–Dawley rats for some of the amino acids surveyed. With the exception of compound **21**, little difference in GT1a potency was observed upon incorporation of various alkyl and cycloalkyl substituents. Conversely, plasma drug exposure depended heavily on the nature of the amino acid substituent. For example, replacement of the C2' phenyl side *D*-Phg residue with an *L*-Val subunit (**20**; Y = (*S*)-*i*Pr) resulted in 20-fold higher compound exposure than analogue **19** (Y = (*R*)-Ph).

The addition of a second *L*-Val group (X = (*S*)-*i*Pr) resulted in even higher plasma drug levels after 10 mg kg<sup>-1</sup> oral dosing. Additionally, compound **22**, which has an *S,S,S,S* configuration, showed 420-fold higher plasma AUC values than its *R,S,S,S* diastereomer **21**. Higher plasma exposures of **22** are presumably due to a transporter that recognizes the *L*-Pro-*L*-Val dipeptide subunit. Further SAR on a variety of homologated valine analogues (that is, cyclobutylglycine **24**, *tert*-butylglycine **25**, homoalanine **26**) showed better exposure than **19**, although each were inferior to **22**.

Cyclopropylglycine analogue **23** displayed similar plasma drug exposure and oral bioavailability in the rat while maintaining good potency in the GT1a and GT1b replicon assays. However, examination of the overall potency profiles of **22** versus **23** showed a significant loss in potency against both GT2a and the key genotype 1a Y93H mutant. As such, compound **22** was selected for early clinical development under the moniker MK-4882 (Table 5).

The synthesis of MK-4882 is straightforward and is illustrated in Schemes 1 and 2. *N*-Boc-*L*-proline aldehyde was converted into the 2-substituted imidazole **22a** using a Radziszewski imidazole synthesis in good yield. Imidazole **22a** was subsequently treated with excess NBS in THF to give the C4,C5-dibrominated intermediate, which was reduced with sodium sulfite to provide the key monobrominated imidazole intermediate **22b**.

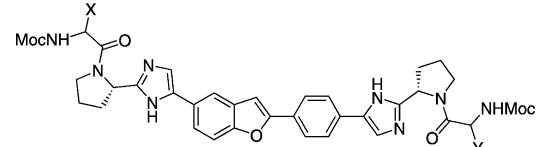
**Table 3.** Imidazole SAR.



Compd	Substituent <sup>[a]</sup>		Genotype, EC <sub>50</sub> [nM] <sup>[b]</sup>			C <sub>max</sub> [μM] <sup>[c]</sup>
	A	B	1b	2a	1a	
16	-(O)CHN-	-NHC(O)-	0.01	0.01	27	0.03
17	imidazole	-NHC(O)-	0.002	0.004	2	0.01
18	-(O)CHN-	imidazole	0.006	0.002	0.3	0.03
19	imidazole	imidazole	0.004	0.004	0.015	0.02

[a] Imidazole = 2-prolyl-substituted imidazole. [b]  $n \geq 3$ . [c] Peak plasma concentration following 10 mg kg<sup>-1</sup> p.o. dose in 10% Tween to fasted male Sprague–Dawley rats (average of  $n = 2$ ).

**Table 4.** Amino acid SAR.



Compd	X	Y	GT1a EC <sub>50</sub> [nM] <sup>[a]</sup>		AUC [μM h <sup>-1</sup> ] <sup>[b]</sup>
			1b	2a	
19	( <i>R</i> )-phenyl	( <i>R</i> )-phenyl	0.015	0.5	10
20	( <i>R</i> )-phenyl	( <i>S</i> )-isopropyl	0.018	10	10
21	( <i>R</i> )-isopropyl	( <i>S</i> )-isopropyl	25	0.1	10
22	( <i>S</i> )-isopropyl	( <i>S</i> )-isopropyl	0.01	42	10
23	( <i>S</i> )-cyclopropyl	( <i>S</i> )-cyclopropyl	0.07	38	10
24	( <i>S</i> )-cyclobutyl	( <i>S</i> )-cyclobutyl	0.14	10	10
25	( <i>S</i> )- <i>tert</i> -butyl	( <i>S</i> )- <i>tert</i> -butyl	0.15	10	10
26	( <i>S</i> )-ethyl	( <i>S</i> )-ethyl	0.02	7.5	10

[a] Values are the average of  $n \geq 3$  experiments. [b] 10 mg kg<sup>-1</sup> p.o. dosed as a homogeneous solution in 10% Tween to fasted male Sprague–Dawley rats (average of  $n = 2$  animals).

**Table 5.** Profiles of compound 22 (MK-4882) and 23.

Compd	Genotype, EC <sub>50</sub> [nM] <sup>[a]</sup>				Rat p.o. <sup>[b]</sup>	
	1b	2a	1a	1aY93H	AUC [μM h <sup>-1</sup> ]	F [%]
22	0.001	0.04	0.009	27	42	38
23	0.003	6.2	0.07	230	38	45

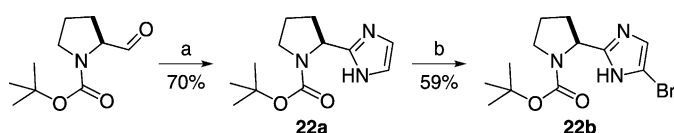
[a]  $N \geq 3$ ; [b] 10 mg kg<sup>-1</sup> p.o. dosed in 10% Tween to fasted male SD rats (average of  $N = 2$ ).

The 2-phenylbenzofuran scaffold was easily prepared via one-pot Cs<sub>2</sub>CO<sub>3</sub>-mediated alkylation/intramolecular cyclocondensation between 5-bromosalicylaldehyde and ethyl-2-bromo-(4-bromophenyl)acetate (**22c**). Metal-halogen exchange of 5-bromo-2-(4-bromophenyl)benzofuran (**22d**) afforded the bis-pinacolboronate ester, which was subsequently coupled to bromoimidazole **22b**. Deprotection of the proline Boc groups afforded penultimate compound **22f**, which was subjected to an amide coupling protocol using the BOP reagent and two equivalents of *N*-Moc-L-Val.

MK-4882 was found to be highly potent against both genotype 1a and 1b, with EC<sub>50</sub> values in the low-picomolar range

and showed only a three- to fourfold shift in the presence of 40% normal human serum. A number of clinical, in vivo, and in vitro studies have identified key mutations that confer resistance to NS5A inhibitors.<sup>[9,10]</sup> These mutations arise principally at residues 28 (1a and 1b), 30 (GT1a), 31 (GT1a and GT1b), and 93 (GT1a and GT1b). MK-4882 potency is shifted to low nanomolar against many mutations at the key NS5A residues 30, 31, and 93. Typically, the magnitude of the potency shift was greater in the GT1a background. For example, MK-4882 potencies against L31V and Y93H mutants in the GT1b background were 0.5 and 3.0 nM, respectively, whereas in the genotype 1a background they were 2 and 27 nM. Data are summarized in Table 6.

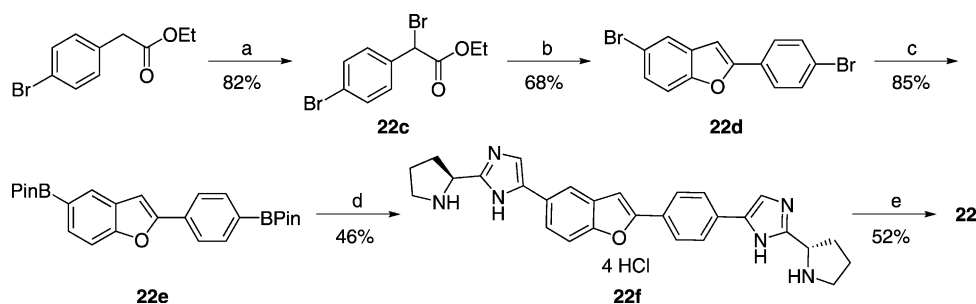
The pharmacokinetic properties of MK-4882 were studied in Sprague–Dawley rats, beagle dogs, and rhesus monkeys. MK-4882 demonstrated low clearance and moderate half-life (2–5 h) in the three species. The oral bioavailability was 26% in dog and 38% in rat, demonstrat-



**Scheme 1.** Synthesis of bromoimidazole fragment **22c**. Reagents and conditions: a) glyoxal, 7 N NH<sub>3</sub> in MeOH; b) 1. NBS, THF, 2. Na<sub>2</sub>SO<sub>3</sub>, EtOH, H<sub>2</sub>O, reflux.

ing that the compound was moderately absorbed in preclinical species. The  $t_{max}$  in both rat and dog was somewhat long, occurring at 4–6 h. MK-4882 demonstrated slightly greater than dose-proportional exposures in rat when dosed at 2 and 100 mg kg<sup>-1</sup> p.o., and also in dog between doses of 1 and 50 mg kg<sup>-1</sup> p.o. Unlike many of the HCV protease inhibitors, MK-4882 did not appear to undergo transport-mediated uptake into liver, as the liver-to-plasma ratio averaged < 10 after oral dosing to rats.

The oral absorption profile in chimpanzees was also evaluated in preparation for in vivo efficacy studies. As such, two male chimpanzees were dosed orally with MK-4882 at 1 mg kg<sup>-1</sup> as a suspension in Tang, and both plasma and liver



**Scheme 2.** Synthesis of MK-4882 (**22**). *Reagents and conditions:* a) NBS, HBr, CCl<sub>4</sub>; b) 5-bromosalicylaldehyde, Cs<sub>2</sub>CO<sub>3</sub>, DMF, reflux; c) bis(pinacolato)diboron, KOAc, Pd(dppf)Cl<sub>2</sub>, dioxane, reflux; d) 1. **22b**, Na<sub>2</sub>CO<sub>3</sub>, Pd(dppf)Cl<sub>2</sub>, THF, H<sub>2</sub>O, reflux, 2. HCl, MeOH; e) *N*-Moc-L-valine, BOP, DIPEA, DMF.

**Table 6.** MK-4882 in vitro potency profile.

Genotype	EC <sub>50</sub> [nM]	Genotype	EC <sub>50</sub> [nM]
1a WT	0.009 ± 0.006	1b WT	0.001 ± 0.001
1a Q30R	7.6 ± 1.1	1b R30Q	0.003 ± 0.001
1a L31V	4.4 ± 3.5	1b L31V	0.39 ± 0.24
1a Y93C	6.6 ± 2.6	1b Y93C	0.004 ± 0.001
1a Y93H	21 ± 3.6	1b Y93H	3.8 ± 1.8
2a WT	0.04 ± 0.01	2b (JFH) <sup>[a]</sup>	286
3a (con1) <sup>[a]</sup>	4.4 ± 0.76	4a (con1) <sup>[a]</sup>	0.31 ± 0.07

[a] Chimeric replicons with indicated NS5A genotype cloned into GT1b (con) or GT2a (JFH) background; see ref. [12] for assay details; values are the means ± SD of *n* > 3 experiments.

levels were determined. Twelve-hour average plasma and liver concentrations were 0.19 and 1.3 μM, respectively. Total free drug concentration in plasma at C<sub>24h</sub> (~3 nM) was greater than the genotype 1b wild-type and genotype 1b mutant EC<sub>50</sub> values (Table 7).

### Pharmacological activity

Both single-dose and multiple-dose studies in chimpanzees chronically infected with HCV were conducted to determine the antiviral efficacy of MK-4882. Study protocols were reviewed and approved by the Institutional Animal Care and Use Committee at both Merck Research Laboratories and at the New Iberia Research Center (University of Louisiana at Lafayette), where the experiments were conducted, to ensure compliance with all federal regulations.

**Table 7.** MK-4882 pharmacokinetics.<sup>[a]</sup>

Species	Cl [mL min <sup>-1</sup> kg <sup>-1</sup> ]	t <sub>1/2</sub> [h]	p.o. C <sub>max</sub> [μM]	p.o. AUC [μM h <sup>-1</sup> ]	F [%]
rat	9.3 ± 0.4	2.0 ± 0.1	0.31 ± 0.11	1.74 ± 0.27	38
dog	6.4 ± 4.0	4.7 ± 0.5	0.19 ± 0.03	1.06 ± 0.06	26
rhesus	9.1	3.0	0.18	1.44	12
chimp	ND	ND	0.45	5.1	ND

[a] Rat, dog, monkey i.v. (1 mg kg<sup>-1</sup>, *n* = 3, 30% captisol + 2 equiv HCl); rat p.o. (2 mg kg<sup>-1</sup>, *n* = 3, 0.5% methylcellulose); dog p.o. (1 mg kg<sup>-1</sup>, *n* = 3, 0.5% methylcellulose); rhesus p.o. (5 mg kg<sup>-1</sup>, *n* = 2, 0.5% methylcellulose); chimpanzee p.o. (1 mg kg<sup>-1</sup>, *n* = 2, Tang); ND: not determined.

A single dose of MK-4882 was orally administered at 1 mg kg<sup>-1</sup> as a suspension in Tang to three chronically infected chimpanzees. Two carried high viral load infections (~10<sup>6</sup> IU mL<sup>-1</sup>) of GT1a or GT1b. The third had a GT1a viral load of 10<sup>4</sup> IU mL<sup>-1</sup> that was homogeneous for the NS3 protease R155K mutation.

All three animals responded rapidly after the single dose; viral load was suppressed an average 2.15 log units within 12 h, with continued suppression to an average nadir of 2.91 log units at 48 h before rebounding. Initial 12 h viral load decreases were similar for both the GT1a and GT1b infections, but an additional one-log suppression was observed with the GT1b infection by 24 h. Suppression of the GT1a infection was maintained through this time but did not increase further (Figure 2).

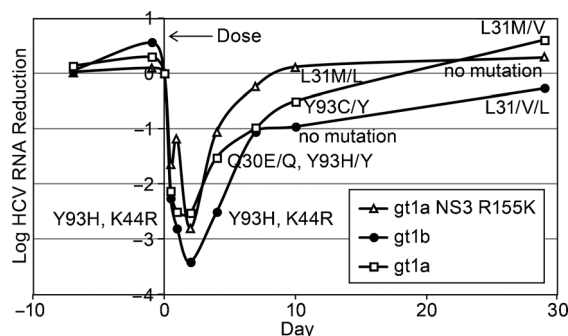


**Figure 2.** MK-4882 single-dose efficacy study: MK-4882 was dosed orally at 1 mg kg<sup>-1</sup> as a suspension in Tang to chronic-HCV-infected chimpanzees harboring GT1a, GT1b, or GT1a NS3 R155K infections. Blood samples were collected periodically, processed to plasma, and evaluated for HCV viral load.

Plasma concentrations of MK-4882 in this study were similar to those found in the satellite study and ranged from 0.06 to 0.17 μM at 12 h, diminishing approximately by half at 24 h. Drug was cleared from plasma and was below the level of quantification (LOQ ~25 nM) by 48 h. The potency of the drug was sufficient to maintain viral suppression through at least 48 h. Drug concentration in the liver, as determined from liver biopsy samples, ranged between 0.77 and 1.56 μM at 12 h. The results are consistent with the satellite PK study in uninfected chimps.

Resistance analysis was conducted by population sequencing of the NS5A gene of viral RNA isolated from serially collected plasma samples. The

GT1b-infected chimp became homogenous for the Y93H mutation after 24 h (sequence could not be generated for the 12 h time point, as no additional sample was available at this time). Viral load was further suppressed another 0.6 log units by 48 h, which suggests suppression of mutant virus. Early rebound virus at day 4 was also homogenous for Y93H, but wild-type virus became the predominant population by day 7. An additional K44R polymorphism, co-encoded with the Y93H virus, was no longer observed at day 10 upon re-emergence of wild-type virus, suggesting that mutant and wild-type virus are two distinct populations. Sequencing of a sample collected on day 28 (four weeks post-dose) showed the emergence of a new mixture of L31V/L virus. A similar late emergence of apparently distinct resistant virus was also observed in the GT1a (wild-type) infected chimpanzee (see below). The reason for these phenomena is currently not understood, and the timing of the emergence of L31L/V virus cannot be further pinpointed, as plasma samples were not collected between days 10 and 28.

Rebound virus from the GT1a (wild-type)-infected chimpanzee was heterogenous for both Q30E and Y93H. By day 7, Y93H was the only mutation detectable, and as a mixed population with wild-type virus. By day 10 this evolved to a mixed population of Y93C and wild-type virus. The shift from Y93H to Y93C coincides with diminishing drug plasma levels and is consistent with the greater loss of potency observed with Y93H than Y93C in vitro. However, by day 28 virus evolved further to an L31M/V mixture. For both the GT1a and 1b infections, wild-type eventually re-emerged as the principle viral population (data not shown).

For the chimpanzee encoding the GT1a NS3 R155K infection, L31M/L was detected as a mixed population at day 10, and only wild-type virus was detected on day 28.

Although MK-4882 exhibited a robust virologic response after a single  $1 \text{ mg kg}^{-1}$  dose, the emergence of mutant virus in the rebound phase warranted further evaluation of efficacy following multi-dose administration. Two different HCV-infected chimpanzees (GT1a and GT1b), both treatment-naïve to NS5A inhibitors, were dosed orally at  $1 \text{ mg kg}^{-1}$  once daily for seven days. The pharmacodynamic responses are shown in Figure 3. Liver biopsies were collected 12 h following the final dose; drug concentrations in liver were 7–15-fold higher than plasma levels, consistent with the findings in the Sprague–Dawley study and suggests that MK-4882 is not selectively retained in liver tissue.

The results from the study showed a rapid and robust response immediately following the initial dose, with an average maximal decrease in viral load by  $\sim 3.5$  log units. The GT1b-infected chimpanzee showed a further decline in viral titer through the duration of the study, reaching a maximal 3.8-log suppression of virus by day 7 before rebounding. Virus was mixed Y93H/Y population at day 10 (three days post-dosing), and eventually became homogenous for wild-type (data not shown).

Although the initial response in the GT1a-infected chimpanzee was robust, viral breakthrough was noted beginning at day 2. This eventually led to a 2-log increase in viral titer

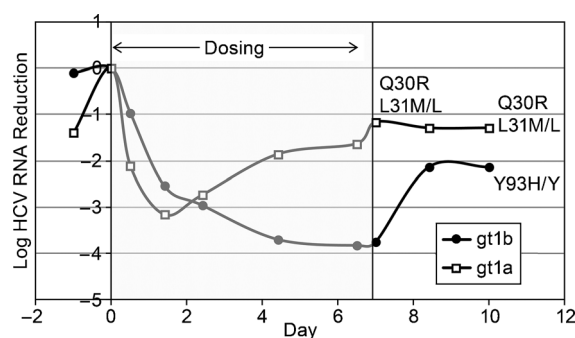


Figure 3. Resistance analysis of the MK-4882 seven-day efficacy study in GT1a- and GT1b-infected chimpanzees.

during dosing, although viral load was still suppressed greater than 1 log from pre-dose levels. Sequence analysis showed that at day 6 virus collected from this animal was heterogenous for both Q30R and L31M/L. A similar viral mixture was observed at day 10 (three days post-dosing). Eventually wild-type virus emerged as the principle population (data not shown).

#### New analogues with improved potency profiles against resistant mutants

The viral breakthrough evidenced in the preclinical proof-of-concept efficacy studies for MK-4882 necessitated the design of newer NS5A inhibitors which had improved virologic profiles against the various genotypes and resistance mutations. SAR of the benzofuran core structure suggested that the introduction of a cyclic constraint could result in more potent inhibitors. The initial strategy involved linking the C3 benzofuran carbon to the C2' phenyl carbon to give tetracyclic core structures **27** and **28** (mode a; Figure 4). Evaluation of these compounds in the replicon assay showed that these modifications resulted in a loss in potency versus the wild-type forms of GT1a and 1b as well as the key mutants L31V and Y93H.

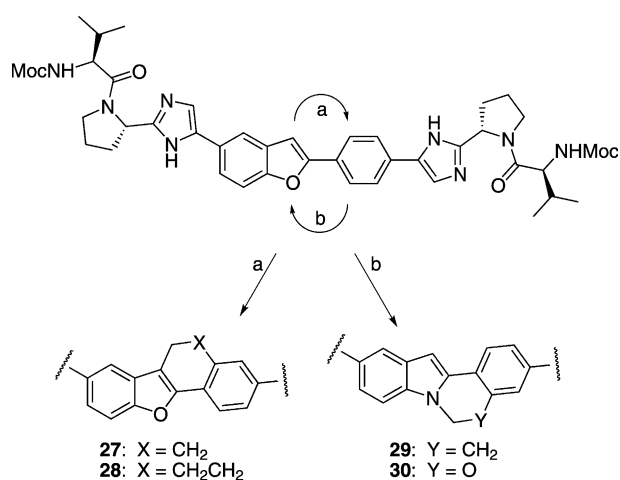


Figure 4. Design strategy for second-generation NS5A inhibitors.

An alternative mode of cyclization (mode b) was examined and was made possible by converting the benzofuran core to an indole scaffold which allowed cyclization from the indole nitrogen to the phenyl C2' carbon through either an ethylene bridge (**29**) or an oxygen-containing bridge (**30**). These modifications afforded inhibitors that possessed a tetracyclic indole scaffold which proved to be equipotent to MK-4882 versus GT1a and GT1b wild-type replicon systems. Further evaluation showed that the GT1a Y93H potency was weakened with the carbon analogue **29** ( $EC_{50}$  = 170 nM). This activity was improved by incorporating an oxygen atom in the two-atom bridge of compound **30** ( $Y = O$ ; GT1a Y93H  $EC_{50}$  = 5 nM). Noteworthy is the fact that the aminal linkage was extremely stable to hydrolytic cleavage even under forcing conditions.

Despite having an improved virologic profile, the unique tetracyclic indole-containing compound **30** proved to be cytotoxic in the low-micromolar range ( $CC_{50}$  ~ 1  $\mu$ M). SAR analysis showed that the addition of a phenyl substituent at C6 abrogated the cytotoxicity. Chiral SFC separation of the two diastereomers afforded the (*S*)-phenyl compound **31** and its *R*-configured epimer **32**. While the virologic profiles of the two diastereomers showed equivalent potency values in the wild-type replicons, compound **31** proved to be 25-fold more potent versus the GT1a Y93H mutant. After extensive profiling, compound **31**, renamed MK-8742, supplanted MK-4882 as our lead clinical compound (Table 8).

MK-8742 was found to be highly potent against most HCV genotypes tested with  $EC_{50}$  values in the low-picomolar range and modest potency shifts in the presence of 40% NHS (Figure 5).

MK-8742 maintained significant potency against most of the NS5A mutations in the screening panel and showed (on average) an order of magnitude improvement relative to MK-4882. MK-8742 potencies against the key L31V and Y93H mutants in the GT1b background were 0.01 and 0.05 nM, respectively, while in the genotype 1a background they were 0.5 and 2 nM. MK-8742 also demonstrated a favorable genotypic virologic profile (Table 9). The decreased potency in the GT2b cell line is attributed to the presence of methionine residue at position 31 of NS5A versus a leucine present in GT2a.<sup>[11]</sup>

The pharmacokinetics of MK-8742 was studied in Wistar Han rats, beagle dogs and cynomolgus monkey. The i.v. clearance was moderate and constituted ~ 14–29% of hepatic blood flow in all three species. The  $V_{d_{ss}}$  was moderate, and the effective half-life was also moderate (2.5–5.9 h). The terminal  $t_{1/2}$  was

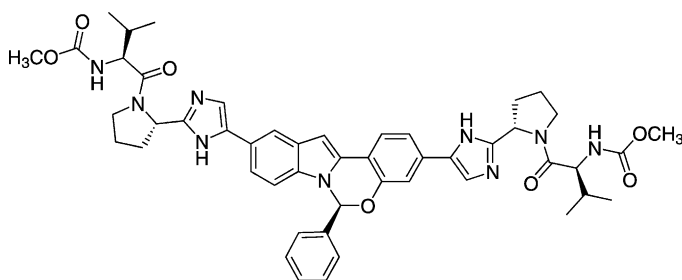


**Figure 5.** Dimethyl ((2*S*,2'*S*)-((2*S*,2'*S*)-2,2'-(5,5'-(*S*)-6-phenyl-6*H*-benzo[5,6]-[1,3]oxazino[3,4-*a*]indole-3,10-diyl)bis(1*H*-imidazole-5,2-diyl))bis-(pyrrolidine-2,1-diyl))bis(3-methyl-1-oxobutane-2,1-diyl)dicarbamate (MK-8742).

**Table 9.** MK-8742 in vitro potency profile GT1-4 and key GT1 mutants.

Genotype	$EC_{50} \pm SD$ [nM]	Genotype	$EC_{50} \pm SD$ [nM]
1a WT	0.004 ± 0.002	1b WT	0.003 ± 0.001
1a Q30H	0.03 ± 0.002	1b L28V	0.004 ± 0.001
1a Q30R	0.5 ± 0.5	1b R30Q	0.009 ± 0.003
1a L31F	0.08 ± 0.04	1b L31F	0.05 ± 0.02
1a L31V	0.5 ± 0.3	1b L31V	0.01 ± 0.01
1a Y93C	0.2 ± 0.07	1b Y93C	0.005 ± 0.001
1a Y93H	2.4 ± 1.3	1b Y93H	0.05 ± 0.03
2a WT	0.003 ± 0.001	2b (JFH) <sup>[b]</sup>	3.4 ± 2.6
3a (con1) <sup>[b]</sup>	0.03 ± 0.01	4a (con1) <sup>[b]</sup>	0.003 ± 0.001

[a] SD is calculated from  $n > 3$  independent experiments. [b] Chimeric replicons with indicated NS5A genotype cloned into GT1b (con1) or GT2a (JFH) background; see ref. [12] for assay details.

longer (4–16 h) than the effective  $t_{1/2}$ , suggesting rate-limited return from tissue compartments. The oral bioavailability was low to moderate (9–35%) for all three species. The low to moderate bioavailability is likely due to limited absorption which is consistent with low passive permeability in MDCKII cells of 47  $\text{nm s}^{-1}$ . Preclinical modeling of MK-8742 suggested a high potential for low-dose once-daily dosing in the clinic (Table 10).

The first-generation synthesis of MK-8742 proceeded in eight linear steps (12 total steps) from commercially available materials with a 3% non-optimized yield from the longest linear sequence (Scheme 3). An improved synthesis which supported early-stage clinical trials has been developed and will be reported elsewhere. Thus, the C2' phenylindole intermediate **31a** was prepared by starting from 5-bromoacetophenone and *p*-bromophenylhydrazine using well-established two-step Fisher indole conditions. The indole NH group was cyclized onto the C2' phenolic group using standard alkylating conditions to give the racemic tetracyclic scaffold **31b** in good overall yield. The dibromide intermediate was subsequently converted into the corresponding pinacolboronate ester **31c** using standard procedures.

Boronate ester **31c** was then coupled with two equivalents of the heterocyclic bromide **22b** in the presence of a catalytic amount of Pd(dppf)Cl<sub>2</sub> followed by work-up and deprotection of the Boc

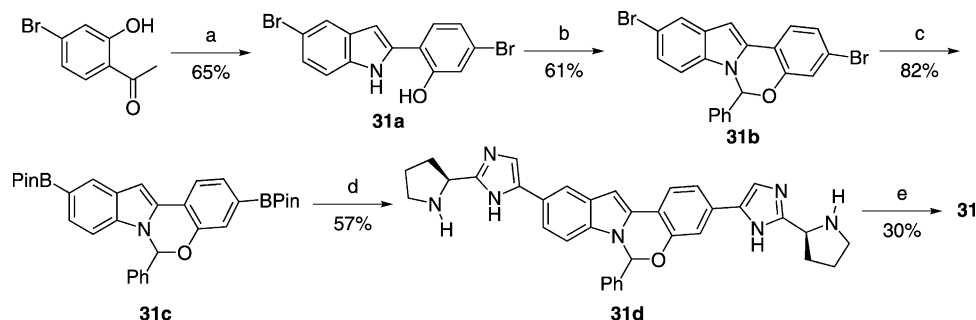
**Table 8.** SAR for tetracyclic inhibitors.<sup>[a]</sup>

Compd	Genotype, $EC_{50}$ [nM]					$CC_{50}$ [ $\mu$ M]
	1b	2a	1a	1aL31V	1aY93H	
<b>22</b>	0.003	0.04	0.01	6	24	9
<b>29</b>	0.02	0.90	0.002	ND	170	1
<b>30</b>	0.001	0.16	0.002	2	5	1
<b>31</b>	0.003	0.003	0.004	0.5	2.4	> 25
<b>32</b>	0.005	0.010	0.002	ND	60	> 25

[a]  $N \geq 3$ ; ND: not determined.

Species	Cl [mL min <sup>-1</sup> kg <sup>-1</sup> ]	t <sub>1/2</sub> [h]	p.o. C <sub>max</sub> [μM]	p.o. AUC [μM h <sup>-1</sup> ]	F [%]
rat <sup>[a]</sup>	24 ± 8.0	4.2 ± 1.0	0.36 ± 0.3	2.3 ± 1.0	~9
dog <sup>[b]</sup>	8.4 ± 2	7.7 ± 2.0	0.29 ± 0.02	1.7 ± 0.3	~35
monkey <sup>[b]</sup>	5.2 ± 0.3	16 ± 4.0	0.1 ± 0.04	1.2 ± 0.4	~17

[a] 5 mg kg<sup>-1</sup> i.v. (3% DMA in 40% HPβCD; 30 mg kg<sup>-1</sup> p.o. (0.4% HPMC in water). [b] 1 mg kg<sup>-1</sup> i.v. (20% HPβCD; 2 mg kg<sup>-1</sup> p.o. (10% T80/90% PEG400).



**Scheme 3.** Synthesis of MK-8742 (**31**). *Reagents and conditions:* a) 1. *p*-bromophenylhydrazine, AcOH, EtOH, reflux, 2. PPA, 110 °C; b)  $\alpha,\alpha$ -dibromotoluene, K<sub>2</sub>CO<sub>3</sub>, DMF, 100 °C; c) bis(pinacolato)diboron, KOAc, Pd(dppf)Cl<sub>2</sub>, dioxane, reflux; d) 1. **22b**, Na<sub>2</sub>CO<sub>3</sub>, Pd(dppf)Cl<sub>2</sub>, THF, H<sub>2</sub>O, reflux, 2. HCl, MeOH; e) *N*-Moc-L-valine, BOP, DIPEA, DMF, then chiral SFC.

groups provided the desired compound **31d** in 57% yield. Amide coupling with *N*-methoxycarbonyl-L-valine afforded compound **31** as a mixture of diastereomers which were easily separated by SFC chromatography. MK-8742 was the second diastereomer to elute and was determined to be the *S,S,S,S* diastereomer by single-compound X-ray analysis. An enantioselective synthesis of the tetracyclic scaffold has since been established and will be reported elsewhere.

## Conclusions

A concerted research effort that combined components from both internal and literature compounds led to a series of benzofuran-based NS5A structures which exhibited good potency versus genotype 1b. A detailed medicinal chemistry effort was undertaken and included the exploration of various amide bond isosteres. This work ultimately led to the incorporation of two imidazole subunits and afforded compounds with subnanomolar EC<sub>50</sub> values against genotypes 1a and 2a. Further optimization of this series using an expanded panel of HCV genotypes and clinically relevant NS5A resistant mutant strains led to the discovery of the early lead compound MK-4882 which showed efficacy in a non-human primate model at a moderate dose. Viral breakthrough with the genotype 1a infected chimpanzee, however, focused attention on developing analogues that were more potent against resistant variants while maintaining or improving the broad genotype profile.

Strategic incorporation of a cyclic constraint and further optimization led to the discovery of MK-8742, a tetracyclic indole-based analogue of MK-4882 which showed both a broad genotypic potency profile and an increased potency against clinical-

ly relevant resistance variants. MK-8742 exhibits antiviral activity against several HCV genotypes (including 1a, 1b, 2a, 3a, 4a) with decreased potency against genotype 2b. Based on its preclinical characterization, this clinical candidate has the potential to retain significant activity against many resistant HCV mutants in both the GT1a and GT1b backgrounds. MK-8742 is currently being evaluated as a component of an all-oral direct-acting antiviral treatment for the cure of HCV. Results from early clinical studies in both healthy volunteers and HCV-infected patients indicate that the favorable preclinical profile of MK-8742 translates into a clinically efficacious drug with broad activity and pharmacokinetics suggestive of moderate once-daily dosing.

## Experimental Section

### Biology

All animal studies were performed according to the NIH Guide for the Care and Use of Laboratory Animals, and experimental protocols were approved by the Merck Institutional Animal Care and Use Committee. The HCV genotype was determined by a line probe assay (Versant HCV genotype assay, LiPa, Bayer Diagnostics/Innogenetics) and confirmed by RT-PCR rescue and sequencing of HCV genetic material.<sup>[12]</sup> HCV-infected chimpanzees were dosed orally at 1 mg kg<sup>-1</sup> for a single dose or q.d. for seven days by the voluntary ingestion of MK-4882 (in a Tang vehicle). Viral load determinations were performed on plasma samples using the HCV TaqMan assay (Cenetrion Diagnostics, Austin, TX, USA). MK-4882 drug concentrations in plasma or liver biopsy specimens were conducted as described above (under pharmacokinetic studies). Viral resistance analysis of chimpanzee plasma samples was conducted similarly to a previously published protocol using NS5A-specific primers.<sup>[13]</sup> Primary screening assays were conducted against gt1b, gt2a, or gt1a replicon cell lines using a luciferase-based reporter assay.<sup>[14]</sup> EC<sub>50</sub> determinations against the panel of genotype or mutant replicon cell lines were conducted using a TaqMan-based assay.<sup>[15]</sup> The NS5A sequences for the genotypes are GT1a (H77), GT1b (con1), GT2a (JFH), GT2b (AB030907), GT3a (NC009824), and GT4a (DQ418742).

### Chemistry

Solvents, reagents, and intermediates that are commercially available were used as received. Reagents and intermediates that were not commercially available were prepared in the manner as described below. <sup>1</sup>H NMR spectra were obtained on a Varian VNMR System 400 (400 MHz) and are reported as ppm downfield from

Me<sub>2</sub>Si with number of protons, multiplicities, and coupling constants in Hz indicated parenthetically. Where LC–MS data are presented, analyses was performed using an Agilent 6110A MSD or an Applied Biosystems API-100 mass spectrometer, and the parent ion is given. Flash column chromatography was performed using pre-packed normal-phase silica from Biotage, Inc. or bulk silica from Fisher Scientific. Unless otherwise indicated, column chromatography was performed using a gradient elution of hexanes/ethyl acetate, from 100% hexanes to 100% ethyl acetate.

### Procedure for the synthesis of MK-4882 (22)

#### (S)-tert-Butyl-2-(1H-imidazol-2-yl)pyrrolidine-1-carboxylate (22a):

To (S)-Boc-prolinal (80.0 g, 0.40 mol) was added a solution of ammonia in MeOH (prepared from 150 mL of 7 N NH<sub>3</sub>/MeOH and 200 mL MeOH, 1.05 mol, 260 mol%). An exotherm was noted with the internal temperature rising to ~30 °C. The solution was allowed to stir for 0.5 h at ambient temperature, then glyoxal (76 g, 0.52 mol) was added over 5 min in portions, with the internal temperature rising to ~60 °C and then returning to room temperature after 1 h. The reaction was allowed to stir for an additional 15 h, and the reaction mixture was concentrated. The resulting residue was diluted with CH<sub>2</sub>Cl<sub>2</sub> (1 L) and H<sub>2</sub>O (0.5 L) was added, and the organic phase was washed with H<sub>2</sub>O (0.25 L), dried over MgSO<sub>4</sub>, filtered and concentrated. The residue obtained was slurried with warm EtOAc (~100 mL) and hexane (100 mL), then was cooled and filtered. The solid obtained was washed with 30% EtOAc/hexane to provide compound **22a** (66.2 g, 70% yield). <sup>1</sup>H NMR (400 MHz, [D<sub>6</sub>]DMSO): δ = 11.6 (brs, 1H), 6.86 (s, 2H), 4.76 (m, 1H), 3.48 (m, 1H), 3.35–3.29 (m, 1H), 2.23–1.73 (m, 4H), 1.15 ppm (s, 9H); <sup>13</sup>C NMR (400 MHz, [D<sub>6</sub>]DMSO): δ = 154.4, 154.0, 150.5, 149.7, 135.8, 79.1, 78.7, 55.7, 55.1, 47.1, 46.8, 33.9, 32.2, 28.8, 28.5, 24.4, 23.6 ppm; MS (ESI) *m/z* 238 [M+H]<sup>+</sup>.

#### (S)-tert-Butyl-2-(4-bromo-1H-imidazol-2-yl)pyrrolidine-1-carboxylate (22b):

To a suspension of compound **22a** (140 g, 0.59 mol) in THF (2000 mL) was added *N*-bromosuccinimide (200 g, 1.1 mol). The mixture was allowed to stir at ambient temperature under N<sub>2</sub> gas for ~15 h. The solvent was then removed in vacuo, and the residue obtained was purified by silica gel chromatography (EtOAc eluent) to provide 230 g of the desired 4,5-dibromoimidazole analogue. *R*<sub>f</sub> = 0.58 (EtOAc/hexanes 2:3); <sup>1</sup>H NMR (400 MHz, CDCl<sub>3</sub>): δ = 10.8 (brs, 1H), 4.74 (s, 1H), 3.38 (s, 2H), 2.81 (m, 1H), 2.1–2.2 (m, 2H), 1.92 (m, 1H), 1.49 ppm (s, 9H); MS (ESI) *m/z* 396 [M+H]<sup>+</sup>. The compound (230 g, 0.58 mol) was suspended in EtOH/H<sub>2</sub>O (1:1 ratio, 3000 mL) and 733 g (5.80 mol). Na<sub>2</sub>SO<sub>3</sub> was added. The resulting mixture was allowed to stir at mild reflux for ~15 h. After cooling to room temperature, the mixture was extracted with CH<sub>2</sub>Cl<sub>2</sub> twice, and the combined organic washings were concentrated to afford a semi-solid. The residue obtained was purified using chromatography on silica gel to provide **22b** (131 g, 70%). *R*<sub>f</sub> = 0.47 (EtOAc/hexanes 2:3); <sup>1</sup>H NMR (400 MHz, [D<sub>6</sub>]DMSO): δ = 12.12 (brs, 1H), 7.10 (m, 1H), 4.70 (m, 1H), 3.31 (m, 1H; overlapped with water signal), 2.25–1.73 (m, 4H), 1.39/1.17 ppm (s, 3.8H + 5.2H); <sup>13</sup>C NMR (400 MHz, [D<sub>6</sub>]DMSO): δ = 154.4, 153.9, 151.0, 150.3, 115.8, 115.4, 113.3, 79.4, 78.9, 55.6, 55.1, 47.1, 46.9, 33.9, 32.3, 28.8, 28.5, 24.4, 23.6 ppm; MS (ESI) *m/z* 317 [M+H]<sup>+</sup>.

**Ethyl 2-bromo-2-(4-bromophenyl)acetate (22c):** To a stirred solution of ethyl 4-bromophenylacetate (50.0 g, 205.8 mmol) in CCl<sub>4</sub> (500 mL) was added NBS (38.0 g, 214.7 mmol) then 48% aqueous HBr (4 drops). After the addition, the solution was stirred overnight at 80 °C under argon. The reaction was cooled, filtered, and concentrated. The resulting oil was directly used the next step without purification. <sup>1</sup>H NMR (400 MHz, CDCl<sub>3</sub>): δ = 7.49 (d, *J* = 8.4 Hz, 2H),

7.42 (d, *J* = 8.6 Hz, 2H), 5.28 (s, 1H), 4.24 (t, *J* = 7.3 Hz, 2H), 1.28 ppm (d, *J* = 7.1 Hz, 3H); <sup>13</sup>C NMR (400 MHz, CDCl<sub>3</sub>): δ = 168.1, 135.1, 135.1, 132.2, 132.2, 130.5, 123.7, 62.9, 45.9, 14.1 ppm.

**5-Bromo-2-(4-bromophenyl)benzofuran (22d):** To a solution of **22c** (2.0 g, 6.2 mmol) in DMF (20 mL) was added 5-bromosalicylaldehyde (1.2 g, 6.0 mmol) and Cs<sub>2</sub>CO<sub>3</sub> (2.0 g, 12.3 mmol) under N<sub>2</sub> protection. The resulting suspension was stirred for 5 h at 160 °C, cooled and treated with water. The resulting precipitate was filtered, and the filtrate cake was dried to give the desired compound **22d** as a white solid which was used directly in next step. *R*<sub>f</sub> = 0.57 (hexane); <sup>1</sup>H NMR: (400 MHz, CDCl<sub>3</sub>): δ = 7.69–7.71 (m, 3H), 7.58 (d, *J* = 8.6 Hz, 2H), 7.35 (m, 2H), 6.95 ppm (s, 1H).

**4,4,5,5-Tetramethyl-2-(4-(5-(4,4,5,5-tetramethyl-1,3,2-dioxaborolan-2-yl)benzofuran-2-yl)phenyl)-1,3,2-dioxaborolane (22e):** A suspension of **22d** (4.43 g, 12.58 mmol), bis(pincolato)diboron (8.31 g, 32.72 mmol), KOAc (3.72 g, 37.7 mmol) and Pd(dppf)Cl<sub>2</sub> (921 mg, 1.26 mmol) in dioxane (100 mL) was heated at reflux for 4 h under a nitrogen atmosphere. The mixture was cooled and concentrated and the residue was partitioned between H<sub>2</sub>O and CH<sub>2</sub>Cl<sub>2</sub>. The aqueous phase was extracted with CH<sub>2</sub>Cl<sub>2</sub> (20 mL × 3), and the combined organic extracts were washed with brine, dried over Na<sub>2</sub>SO<sub>4</sub> then concentrated. The residue was purified by chromatography on silica gel (EtOAc/hexanes 1:4) to afford the desired compound (5.0 g, 85%). <sup>1</sup>H NMR: (400 MHz, CDCl<sub>3</sub>): δ = 8.12 (s, 1H), 7.86–7.94 (m, 4H), 7.79 (d, *J* = 8.4 Hz, 1H), 7.55 (d, *J* = 8.4 Hz, 1H), 7.12 (s, 1H), 1.41 (s, 12H), 1.39 ppm (s, 12H).

**2-((S)-Pyrrolidin-2-yl)-5-(4-(5-(2-((S)-pyrrolidin-2-yl)-1H-imidazol-5-yl)benzofuran-2-yl)phenyl)-1H-imidazole (22f):** A suspension of bromoimidazole **22b** (1.58 g, 5.0 mmol), boronate ester **22e** (892 mg, 2.0 mmol), Pd(dppf)Cl<sub>2</sub> (146 mg, 0.20 mmol), and Na<sub>2</sub>CO<sub>3</sub> (636 mg, 6.0 mmol) were held at reflux in THF/H<sub>2</sub>O (10:1, 33 mL) overnight under N<sub>2</sub> protection. The mixture was cooled and filtered. The filtrate was washed with water (50 mL) then extracted with EtOAc (100 mL). The organic phase was removed and washed with brine (20 mL) then dried over anhydrous Na<sub>2</sub>SO<sub>4</sub>. The solution was concentrated, and the resulting residue was purified by column chromatography (petroleum ether/EtOAc = 8:1 → 5:1) to afford the desired compound. MS (ESI) *m/z* 641 [M+H]<sup>+</sup>. The product was added into 3 M HCl/CH<sub>3</sub>OH (20 mL) and the mixture was stirred at RT for 3 h. The mixture was concentrated and the crude product was used directly in the next step without further purification. <sup>1</sup>H NMR (400 MHz, [D<sub>6</sub>]DMSO): δ = 10.5 (brs, 1H), 10.1 (brs, 1H), 8.3 (s, 1H), 8.25 (m, 2H), 8.05–8.15 (m, 5H), 7.92 (dd, *J* = 1.8, 6.8 Hz), 7.81 (d, *J* = 6.8 Hz, 7.64 (s, 1H), 5.12 (t, *J* = 8.4 Hz, 1H), 5.09 (t, *J* = 8.3 Hz, 1H), 3.35–3.53 (m, 4H), 2.53–2.61 (m, 6H), 2.19–2.29 ppm (m, 2H); <sup>13</sup>C NMR (400 MHz, [D<sub>6</sub>]DMSO): δ = 156.6, 155.0, 143.0, 142.2, 135.0, 130.1, 129.9, 126.4, 126.1, 123.7, 123.4, 118.9, 117.6, 116.4, 112.6, 103.5, 53.4, 53.0, 46.2, 46.1, 30.2, 30.1, 24.8, 24.7 ppm; MS (ESI) *m/z* 441 [M+H]<sup>+</sup>.

**MK-4882 (22):** To a mixture of proline analogue **22f** (440 mg, 1.0 mmol), *N*-Moc-L-valine (367 mg, 2.1 mmol) and DIPEA (0.4 mL) in DMF (3 mL) was added BOP reagent (968 mg, 2.2 mmol). The resulting mixture was stirred at RT for 16 h. The solution was subjected directly to reversed-phase HPLC to afford 405 mg (52%) of the desired compound **22**; mp: 130–131 °C; <sup>1</sup>H NMR (400 MHz, CD<sub>3</sub>OD): δ = 7.7–8.1 (m, 10H), 7.4 (m, 1H), 5.3 (m, 2H), 4.3 (m, 2H), 4.1 (d, *J* = 4.8 Hz, 2H), 3.9 (m, 2H), 3.7 (m, 6H), 2.6 (d, *J* = 4.8 Hz, 2H), 2.0–2.4 (m, 8H), 1.3–1.4 (m, 2H), 0.9–1.0 ppm (m, 12H); <sup>13</sup>C NMR (400 MHz, [D<sub>6</sub>]DMSO): δ = 170.9, 157.3, 156.1, 153.5, 149.9, 149.4, 139.9, 139.1, 129.7, 127.6, 125.2, 125.0, 116.4, 113.6, 112.1,

111.2, 101.8, 58.5, 54.7, 51.9, 31.3, 30.3, 24.7, 19.5, 19.0 ppm; MS (ESI)  $m/z$  780  $[M+H]^+$ .

### Procedure for the synthesis of MK-8742

**5-Bromo-2-(5-bromo-1H-indol-2-yl)phenol (31 a):** A mixture of 5'-bromo-2'-hydroxyacetophenone (4.2 g, 20 mmol) and 4-bromophenyl hydrazine hydrochloride (4.4 g, 20 mmol) in AcOH and EtOH (1:10, 100 mL) was heated at reflux and allowed to stir at this temperature for 6 h. The reaction mixture was cooled to room temperature and concentrated to provide 7.2 g (94%) of the desired hydrazone as a solid. The hydrazone was subsequently covered in PPA and heated at 80 °C for 2 h. The reaction mixture was cooled to room temperature and poured into iced water. The resulting solution was extracted with  $CH_2Cl_2$  and the organic extract was washed with brine, dried over  $Na_2SO_4$ , filtered and concentrated. The residue was purified using column chromatography (2:3 EtOAc/hexanes) to provide **31 a** (4.8 g, 65%).  $R_f=0.70$  (EtOAc/hexanes 2:3);  $^1H$  NMR (400 MHz,  $[D_6]DMSO$ ):  $\delta=11.3$  (s, 1H), 10.7 (s, 1H), 7.70 (m, 2H), 7.42 (d,  $J=8.6$  Hz, 1H), 7.19 (m, 2H), 7.11 (dd,  $J=2.0, 8.4$  Hz, 1H), 6.98 ppm (d,  $J=2.0$  Hz, 1H);  $^{13}C$  NMR (400 MHz,  $[D_6]DMSO$ ):  $\delta=154.2, 134.5, 133.9, 128.9, 127.9, 122.5, 121.1, 120.7, 119.4, 117.8, 116.7, 112.1, 110.4, 99.8$  ppm; MS (ESI)  $m/z$  368  $[M+H]^+$ .

**3,10-Dibromo-6-phenyl-6H-benzo[5,6][1,3]oxazino[3,4-a]indole (31 b):** A mixture of **31 a** (1.1 g, 3.0 mmol),  $\alpha, \alpha$ -dibromotoluene (2.25 g, 9.0 mmol) and  $K_2CO_3$  (1.2 g, 9.0 mmol) in 15 mL of DMF was heated at 100 °C and allowed to stir at this temperature for 3 h. The reaction mixture was cooled to room temperature, concentrated, and the residue obtained was dissolved with  $CH_2Cl_2$  and water. The aqueous phase was extracted with  $3 \times 20$  mL of  $CH_2Cl_2$ . The combined organic extracts were washed with brine, dried over  $Na_2SO_4$ , filtered and concentrated. The resulting residue was purified using flash column chromatography on silica gel to provide **31 b** (830 mg, 61%) as a white solid.  $R_f=0.65$  (EtOAc/hexanes 5:95);  $^1H$  NMR (400 MHz,  $CDCl_3$ ):  $\delta=7.72$  (brs, 1H), 7.44–7.46 (d,  $J=8.4$  Hz, 1H), 7.21–7.28 (m, 3H), 7.09–7.12 (m, 3H), 7.04 (s, 1H), 6.99–7.01 (brs,  $J=6.8$  Hz, 2H), 6.78 (s, 1H), 6.63–6.65 ppm (d,  $J=8.4$  Hz, 1H);  $^{13}C$  NMR (400 MHz,  $CDCl_3$ ):  $\delta=150.2, 136.4, 134.1, 132.3, 130.9, 130.1, 129.2, 127.1, 126.6, 125.8, 125.3, 123.6, 122.6, 121.5, 117.2, 114.3, 111.4, 97.0, 84.7$  ppm; MS (ESI)  $m/z$  456  $[M+H]^+$ .

**6-Phenyl-3,10-bis(4,4,5,5-tetramethyl-1,3,2-dioxaborolan-2-yl)-6H-benzo[5,6][1,3]oxazino[3,4-a]indole (31 c):** To a solution of compound **31 b** (456 mg, 1.0 mmol) in 1,4-dioxane was added bis(pinacolato)diboron (559 mg, 2.2 mmol), Pd(dppf)Cl<sub>2</sub> (0.04 mmol), and KOAc (392 mg, 4.0 mmol). The reaction mixture was heated at 110 °C under a blanket of  $N_2$  for 3 h. The reaction mixture was cooled to room temperature, concentrated, and the residue obtained was purified using column chromatography on silica gel (7:3 EtOAc/hexanes) to provide **31 c** (590 mg, 87% yield).  $R_f=0.42$  (EtOAc/hexanes 1:4);  $^1H$  NMR (400 MHz,  $CDCl_3$ ):  $\delta=8.13$  (s, 1H), 7.60 (d,  $J=7.6$  Hz, 1H), 7.52 (d,  $J=8.0$  Hz, 1H), 7.36–7.39 (m, 1H), 7.14–7.19 (m, 4H), 6.93–6.95 (m, 3H), 6.90 (s, 1H), 1.26–1.29 ppm (s, 24H);  $^{13}C$  NMR (400 MHz,  $CDCl_3$ ):  $\delta=148.7, 137.5, 137.3, 131.7, 129.5, 129.3, 129.0, 128.9, 128.9, 128.8, 126.9, 124.3, 123.4, 121.0, 109.1, 98.4, 84.1, 84.0, 83.8, 83.7, 32.1, 25.2, 25.1, 25.0, 14.3$  ppm; MS (ESI)  $m/z$  550  $[M+H]^+$ .

**6-Phenyl-3,10-bis(2-((S)-pyrrolidin-2-yl)-1H-imidazol-5-yl)-6H-benzo[5,6][1,3]oxazino[3,4-a]indole (31 d):** A suspension of compound **31 c** (550 mg, 1.0 mmol), compound **22 b** (760 mg, 2.4 mmol), Pd(dppf)Cl<sub>2</sub> (200 mg),  $Na_2CO_3$  (318 mg, 3.0 mmol) in THF/ $H_2O$  (10:1, 33 mL) was allowed to stir at reflux for 15 h under

$N_2$ . The reaction mixture was cooled to room temperature, filtered, and the filtrate was washed with water (50 mL) then extracted with EtOAc (100 mL). The organic extract was washed with brine, dried over anhydrous  $Na_2SO_4$ , filtered and concentrated. The resulting residue was purified using column chromatography on silica gel (EtOAc) to provide **31 d** (460 mg). MS (ESI)  $m/z$  768  $[M+H]^+$ . The compound was dissolved in 5 mL of MeOH and added to HCl/ $CH_3OH$  (5 mL, 3 M). The resulting reaction was allowed to stir at room temperature for 3 h then concentrated to provide the amine salt (409 mg, 57%), which was used without further purification.  $^1H$  NMR (400 MHz,  $[D_6]DMSO$ ):  $\delta=11.9$  (brs, 1H), 11.1 (brs, 1H), 7.9 (s, 1H), 7.75 (m, 1H), 7.69 (s, 1H), 7.33–7.65 (m, 4H), 7.22–7.30 (m, 4H), 6.93–7.05 (m, 3H), 4.72 (m, 1H), 3.75 (m, 2H), 2.09–2.19 (m, 2H), 1.84–2.02 (m, 4H), 1.0–1.15 ppm (m, 6H); MS (ESI)  $m/z$  568  $[M+H]^+$ .

**MK-8742 (31):** To a solution of **31 d** (300 mg, 0.53 mmol), *N*-methoxycarbonyl-L-valine (185 mg, 1.05 mmol) and DIPEA (0.7 mL, 4.2 mmol) in  $CH_3CN$  (5 mL) was added BOP reagent (515 mg, 1.1 mmol). The resulting reaction was allowed to stir at room temperature and monitored by LC-MS. After LC-MS showed the starting material to be consumed, the reaction mixture was filtered and the filtrate was purified by reversed-phase HPLC to provide crude compound **31** as a mixture of diastereomers (300 mg).  $^1H$  NMR (400 MHz,  $CD_3OD$ ):  $\delta=7.94$  (s, 1H), 7.85 (d,  $J=8.0$  Hz, 1H), 7.74 (s, 1H), 7.63 (s, 1H), 7.48 (s, 1H), 7.35–7.37 (m, 2H), 7.31 (s, 1H), 7.17–7.18 (m, 4H), 7.11 (s, 1H), 6.96–6.98 (d,  $J=7.6$  Hz, 2H), 5.09–5.17 (m, 2H), 4.13 (t,  $J=8.0$  Hz, 2H), 3.99 (brs, 2H), 3.78 (brs, 2H), 3.56 (s, 6H), 2.44–2.47 (m, 2H), 1.92–2.19 (m, 8H), 0.77–0.85 ppm (m, 12H); MS (ESI)  $m/z$  882  $[M+H]^+$ . The diastereomers were separated on a chiral SFC column to afford compound **31** (140 mg, 30%) and the C6 epimer **32** (145 mg, 31%).

**MK-8742 (31):** mp: 160–161 °C;  $R_f=0.46$  (MeOH/ $CH_2Cl_2$  1:9);  $^1H$  NMR (400 MHz,  $CD_3OD$ ):  $\delta=7.90$  (s, 1H), 7.81–7.83 (m, 1H), 7.72 (s, 1H), 7.62 (s, 1H), 7.45 (s, 1H), 7.14–7.33 (m, 6H), 7.09 (s, 1H), 6.93–6.95 (m, 2H), 5.06–5.14 (m, 2H), 3.71–4.11 (m, 6H), 3.52 (s, 6H), 2.41–2.44 (m, 2H), 1.90–2.15 (m, 8H), 0.74–0.86 ppm (m, 12H);  $^{13}C$  NMR (400 MHz,  $[D_6]DMSO$ ):  $\delta=171.0, 157.4, 149.6, 138.3, 134.6, 129.8, 129.5, 127.0, 116.2, 83.5, 58.6, 54.9, 52.1, 47.5, 31.6, 30.5, 24.9, 19.6, 19.2$  ppm; MS (ESI)  $m/z$  882  $[M+H]^+$ .

**MK-8742 diastereomer (32):**  $R_f=0.46$  (MeOH/ $CH_2Cl_2$  1:9);  $^1H$  NMR (400 MHz,  $CD_3OD$ ):  $\delta=8.08$  (s, 1H), 7.91–7.93 (m, 1H), 7.72 (s, 1H), 7.56 (s, 1H), 7.24–7.43 (m, 7H), 7.19 (s, 1H), 7.03–7.05 (m, 2H), 5.16–5.24 (m, 2H), 3.81–4.21 (m, 6H), 3.62 (s, 6H), 2.52–2.54 (m, 2H), 2.00–2.25 (m, 8H), 0.84–0.91 ppm (m, 12H); MS (ESI)  $m/z$  882  $[M+H]^+$ .

**Keywords:** antiviral agents • hepatitis C • inhibitors • medicinal chemistry • structure–activity relationships

- [1] D. Lavanchy, *Clin. Microbiol. Infect.* **2011**, *17*, 107–115.
- [2] T. K. H. Scheel, C. M. Rice, *Nat. Med.* **2013**, *19*, 837–849.
- [3] J. Guedj, H. Dahari, L. Rong, N. D. Sansone, R. E. Nettles, S. J. Cotler, T. J. Layden, S. L. Uprichard, A. S. Perelson, *Proc. Natl. Acad. Sci. USA* **2013**, *110*, 3991–3996.
- [4] a) M. Gao, R. E. Nettles, M. Belema, L. B. Snyder, V. N. Nguyen, R. A. Friedell, M. H. Serrano-Wu, D. R. Langley, J.-H. Sun, D. R. O'Boyle, J. A. Lemm, C. Wang, J. O. Knipe, C. Chien, R. J. Colonna, D. M. Grasela, N. A. Meanwell, L. G. Hamann, *Nature* **2010**, *465*, 96–100; b) R. E. Nettles, M. Gao, M. Bifano, E. Chung, A. Persson, T. C. Marbury, R. Goldwater, M. P. DeMicco, M. Rodriguez-Torres, A. Vutikullird, E. Fuentes, E. Lawitz, J. C. Lopez-Talavera, D. M. Grasela, *Hepatology* **2011**, *54*, 1956–1965.
- [5] a) A. Lok, *Clin. Liver Dis.* **2013**, *17*, 111–121; b) J.-M. Pawlotsky, *J. Hepatol.* **2013**, *59*, 375–382; c) O. Belda, P. Targett-Adams, *Virus Res.* **2012**, *170*,

- 1–14; d) D. G. Cordek, J. T. Bechtel, A. T. Maynard, W. M. Kazmierski, C. E. Cameron, *Drugs Future* **2011**, *36*, 691–711; e) U. Schmitz, S.-L. Tan, *Rec. Patents Anti-Infect. Drug Discovery* **2008**, *3*, 77–92.
- [6] I. Conte, C. Giuliano, C. Ercolani, F. Narjes, U. Koch, M. Rowley, S. Altamura, R. De Francesco, P. Neddermann, G. Migliaccio, I. Stansfield, *Bioorg. Med. Chem. Lett.* **2009**, *19*, 1779–1783.
- [7] M. Serrano-Wu, M. Belema, L. B. Snyder, N. A. Meanwell, D. R. St. Laurent, R. Kakarla, V. N. Nguyen, Y. Qiu, X. Yang, J. E. Leet, M. Gao, D. R. O'Boyle, J. A. Lemm, F. Yang (Bristol-Meyers Squibb), US Pat. Appl. US 20060276511 A1 20061207, **2006**.
- [8] a) J. A. Lemm, D. J. E. Leet, D. R. O'Boyle, J. L. Romine, X. S. Huang, D. R. Schroeder, J. Alberts, J. L. Cantone, J.-H. Sun, P. T. Nower, S. W. Martin, M. H. Serrano-Wu, N. A. Meanwell, L. B. Snyder, M. Gao, *Antimicrob. Agents Chemother.* **2011**, *55*, 3795–3802; b) J. L. Romine, D. R. St. Laurent, J. E. Leet, S. W. Martin, M. H. Serrano-Wu, F. Yang, M. Gao, D. R. O'Boyle, J. A. Lemm, J.-H. Sun, P. T. Nower, X. Huang, M. S. Deshpande, N. A. Meanwell, L. B. Snyder, *ACS Med. Chem. Lett.* **2011**, *2*, 224–229.
- [9] E. J. Lawitz, D. Gruener, J. M. Hill, T. Marbury, L. Moorehead, A. Mathias, G. Cheng, J. O. Link, K. A. Wong, H. Mo, J. G. McHutchinson, D. M. Brainard, *J. Hepatol.* **2012**, *57*, 24–31.
- [10] J. A. Lemm, D. R. O'Boyle, M. Liu, P. T. Nower, R. Colonno, M. S. Deshpande, L. B. Snyder, S. W. Martin, D. R. St Laurent, M. H. Serrano-Wu, J. L. Romine, N. A. Meanwell, M. Gao, *J. Virol.* **2010**, *84*, 482–491.
- [11] T. K. H. Scheel, J. M. Gottwein, L. S. Mikkelsen, T. B. Jensen, J. Bukh, *Gastroenterology* **2011**, *140*, 1032–1042.
- [12] S. S. Carroll, S. W. Ludmerer, L. Handt, K. Koeplinger, N. R. Zhang, D. Graham, M. E. Davies, M. MacCoss, D. J. Hazuda, D. B. Olsen, *Antimicrob. Agents Chemother.* **2009**, *53*, 926–934.
- [13] S. W. Ludmerer, D. J. Graham, M. Patel, K. Gilbert, M. Stahlhut, D. B. Olsen, *J. Virol. Methods* **2008**, *151*, 301–307.
- [14] J. M. Vrolijk, A. Kaul, B. E. Hansen, V. Lohmann, B. L. Haagmans, S. W. Schalm, R. Bartenschlager, *J. Virol. Methods* **2003**, *110*, 201–209.
- [15] N. J. Liverton, S. S. Carroll, J. DiMuzio, C. Fandozzi, D. J. Graham, D. Hazuda, M. K. Holloway, S. W. Ludmerer, J. A. McCauley, C. J. McIntyre, D. B. Olsen, M. T. Rudd, M. Stahlhut, J. P. Vacca, *Antimicrob. Agents Chemother.* **2010**, *54*, 305–311.

---

Received: August 22, 2013

Published online on October 14, 2013